Journal of Solid Mechanics Vol. 10, No. 2 (2018) pp. 364-386

Optimal Locations on Timoshenko Beam with PZT S/A for Suppressing 2Dof Vibration Based on LQR-MOPSO

M. Hasanlu , A. Bagheri *

Department of Mechanical Engineering, Faculty of Engineering, University of Guilan, Rasht, Iran

Received 9 March 2018; accepted 9 May 2018

ABSTRACT

Neutralization of external stimuli in dynamic systems has the major role in health, life, and function of the system. Today, dynamic systems are exposed to unpredicted factors. If the factors are not considered, it will lead to irreparable damages in energy consumption and manufacturing systems. Continuous systems such as beams, plates, shells, and panels that have many applications in different industries as the main body of a dynamic system are no exceptions for the damages, but paying attention to the primary design of model the automatic control against disturbances has highly met the objectives of designers and also has saved much of current costs. Beam structure has many applications in constructing blades of gas and wind turbines and robots. When it is exposed to external loads, it will have displacements in different directions. Now, it is the control approach that prevents from many vibrations by designing an automated system. In this study, a cantilever beam has been modeled by finite element and Timoshenko Theory. Using piezoelectric as sensor and actuator, it controls the beam under vibration by LQR controller. Now, in order to increase controllability of the system and reduce the costs, there are only spots of the beam where most displacement occurs. By controlling the spots and applying force on them, it has the most effect on the beam. By multi-objective particle swarm optimization or MOPSO algorithm, the best weighting matrices coefficients of LQR controller are determined due to sensor and actuator displacement or the beam vibration is controlled by doing a control loop.

Keywords : Vibration attenuation; Timoshenko beam; Optimal placement; PZT patches; LQR controller; Multi-objective particle swarm optimization.

1 INTRODUCTION

PIEZOELECTRIC as sensor and actuator has had a significant application in different industries due to simultaneous direct (sensor) and adverse (actuator) behavior. Piezoelectric shows different unique features in sensor and actuator. The characteristics are high sensitivity due to applying force, high energy storage, vibration absorb, unlimited accuracy, producing great force, rapid transfer of voltage, lack of being influenced by magnetic field, power saving, lack of corrosion and abrasion, working in high temperatures, vacuum compatibility, etc. Due to these features, designers of smart structures use piezoelectric to control structures such as beams, plates, shells,

*Corresponding author.
E-mail address: Bagheri@guilan.ac.ir (A. Bagheri).

trusses, panels, frames, etc., which have wide applications in robots and machines. Optimization design attempts to reduce damages and costs and increase life of these structures by using optimizing the location of sensor, actuator, and controller.

S.T. Quek et al. investigated the vibration suppression of multilayer composite plate as cantilever and four sides clamped and find the best place for locating the piezoelectric sensor and actuator. By using finite element, they completed a numerical modeling. By using two perspectives, one of them based on controllability of mode and the other based on controllability of intelligent system, they extracted the objective function.

Finally, they used Direct Pattern Search method (DPS) to optimize these objective functions and presented their results [1]. W. Liu et al. optimized the location of the piezoelectric sensor and actuator by using H_2 controller and genetic algorithm. During the simulation of their model, they used H_2 soft performance index as a good performance index in order to control the vibration of a plate with two simply supports [2]. H.Y. Guo et al. conducted the optimal placement of piezoelectric sensor and actuator on a truss structure by using genetic algorithm. Their objective was to keep this structure safe against external stimuli; it means that their objective function was considered according to the fault detection in system. But they implemented several reforms and suggestions in genetic algorithm: firstly, they used penalty function method. Second, they used force mutation method to increase the convergence rate of algorithm to the most efficient possible locations for placement of piezoelectric [3]. T.L. Da Rocha et al. conducted the optimal placement of piezoelectric on a cantilever plate as sensor and actuator by using H_{00} soft concept. Modeling of structure was done by using finite element with ANSYS and MATLAB software by using H_∞ and Linear Matrix Inequalities (LMI) method, they calculated the location of sensor and actuator on structure which finally resulted in vibration suppression due to the optimal placement of piezoelectric [4]. S.L dos. Santos e Lucato et al. generally conducted the optimal placement of piezoelectric sensor and actuator on a truss structure called Kagome Truss and their optimization algorithm included annealing and genetic algorithms and had good results from this research [5]. M.Brasseur et al. conducted the optimal placement of piezoelectric on an acoustic structure called Wooden Shutter Box by using controllability gramian index.

The modeling method of this structure included finite element. The objective of this experimental and theoretical research was reaching desirable coordinates for the placement of piezoelectric in order to absorb sound in the room's environment [6]. H.H.Ning in an article investigated and optimized the place and number of piezoelectric on a cantilever plate as sensor and actuator to control the undesirable vibrations in the structure. In order to search the working environment of cantilever plate, genetic algorithm was used to find the best location of piezoelectric sensor and actuator [7]. A.S.D. Oliveira et al. conducted the optimal placement of piezoelectric sensor and actuator patches to form an intelligent structure on a simply support beam by using classic optimization. They extracted the critical coordinates by deriving figure function and put it equal to zero and by the placement of piezoelectric on these specific coordinates, they controlled its vibration.

For controlling the system, they used Singular Value Decomposition (SVD) method as the objective function [8]. S.Y. Wang et al. optimized the location of piezoelectric sensor and actuator on a cantilever plate. In this research, they considered piezoelectric sensor and actuator as isotropic and anisotropic so that can damp torsional vibrations of a composite plate. Modeling of composite plate was used through finite element which was based on the first order shear method and genetic algorithm was used to conduct the optimization process [9]. J. Lottin et al. in a descriptive article studied the optimal placement piezoelectric sensor and actuator on a structure. During four sections, they described placement methods, type of actuator and sensor in terms of efficiency and performance, type of structure, methods of assembling piezoelectric on a structure, methods of controlling system and place optimization criteria [10]. C. Swann et al. by exclusive placement of piezoelectric sensor on a composite plate with boundary conditions of cantilever and four sides clamped, tried to find delamination phenomenon in structure due to vibration. Modeling structure was done by using finite element based on Refined Layer-wise Theory (RLWT). For conducting the optimization process for the place and number of sensors, genetic algorithm and Monte-Carlo Method was used to produce the initial population. Their objective was a troubleshooting method due to the optimal location of piezoelectric sensor for detection of composite delamination because of receiving voltage signals and comparing it to the non-delamination situation [11].

A.Belloli et al. analyzed the placement of piezoelectric ceramic pieces to neutralize the vibrations in rear wings of a race car. Optimization was done by using CATIA V5, ANSYS 9.0 and DynOPS software and it was completely designed and analyzed. The objective of optimization in this research was finding the best size, place and direction for the placement of piezoelectric and interesting results were extracted [12]. Zhi-Cheng. Qiu in their article studied cantilever plate model analytically and by using controllability degree and observability index of system, they optimized the placement of piezoelectric for vibration depression of structure. In this article, they tried to control the vibration of plate by combining two control methods including PPF and PDC (Proportional Derivative Control). The

type of studied vibration was torsional and flexural vibration. By making the torsional and flexural coupling relations independent through Bandwidth Butterworth Filter (BBF) method, they analyzed the vibration of system and applied controlling rules on them [13]. T. Roy et al. conducted a research on the optimal placement of piezoelectric patches by using genetic optimization algorithm and quadratic optimal control or LQR method. Their studied structures included Spherical composite panel, a cantilever composite beam and a composite plate. One of the innovations in this study was using multilayered piezoelectric composite pieces as sensor and actuator. By incorporating LRQ method and algorithm, it can be said that in LQR method, 3 coefficients in R and Q fixed matrixes are defined and by using genetic algorithm, the most optimized answer for these three coefficients is obtained.

Finally, by the placement of these coefficients in energy relationship, the best places for actuator and sensor can be suggested [14]. M.R. Safizade et al. studied the optimal place for a plate with all edges clumped by using controllability gramian performance index and genetic algorithm. Structural equations of plate were extracted analytically and were incorporated with analytical equations of piezoelectric actuator and the equation of an intelligent structure was obtained. Then by using a controlling method, the optimal placement of their system was conducted. In this method, the main responsibility is system's controllability and expressing an optimum control input so that by applying forces on this optimal place of structure, system, can be damped [15]. J. Yang et al. in two researchers studied the optimal placement of piezoelectric sensor and actuator on a plate. Their theory was that in order to increase the controlling performance of system or in other words controlling the system by piezoelectric results in vibration suppression, piezoelectric actuator should affect a specific direction on plate. Now there are coordinates on the plate that show their potential effect by the placement of piezoelectric actuator and system is controlled more efficiently. They used two types of Simulated Annealing for the TSP (SATSP) algorithm and another algorithm called Hopfield-Tank for the TSP (HTTSP) to optimize the place of plate. The results of SATSP optimization algorithm were better than HTTSP. In this article, by using SATSP algorithm alongside Genetic Algorithm for TSP (GATSP) algorithm, better results from GATSP were provided compared to SATTSP [16-17].

The structure studied in this paper is a uniform cantilever beam with a rectangular cross-section. The beam has been under vibration due to non-periodic inputs. The beam goes under vibration by applying transverse load. Using a piezoelectric sensor and actuator, MOPSO optimization algorithm and LQR controller found the best coefficients of the matrices Q and R and the optimum location and control operations are done on it, which finally control the structure from unwanted vibrations.

2 PIEZOELECTRIC MATERIAL

2.1 Sensors

Sensors are generally composed of strain gauges, accelerators, optical fibers, piezoelectric layer, and piezo ceramics. Piezoelectric materials are used as both strain sensors and sensors measuring strain rate to receive vibrations. Sensors transform strain and displacement to electric filed. Piezoelectric sensors are usually made of polymers such as PVDF and are very soft. They can easily transform to thin plates and stick on surface. The key factors for sensors are their sensitivity to strain, displacement, and their size. The sensors used in structures such as shells and plates are known as PZT. When mechanical stress is applied on a piezo ceramic plate in the longitudinal direction (parallel to polarization), a voltage is produced that tries to bring back the initial thickness to the patch. Similarly, when a mechanical stress is applied in the direction perpendicular to the polarization, a voltage is produced that tries to bring back the initial width and length. Multi-layer sensors are composed of many piezoelectric layers that are constructed as a huge structure with high capacity and are used to measure strong forces and generating high voltage.

2.2 Actuators

Smart actuators are usually made of piezoelectric materials, smart alloys, and electrostrictives. In most cases, they change electric input to strain or displacement. Piezoelectric and electrostrictives are available in the form of ceramic and smart alloys as metal alloys. Piezoelectric are also available as thin polymeric layers. What separates piezoelectricity from electrostrictive is that piezoelectric materials can have both increase and decrease in length proportional to field direction. The total strain generated in the actuator is equal to the sum of mechanical strains resulted from electrical field strains and stresses. Actuators can be divided in terms of function into lamina and laminate actuators. Piezoelectric actuators can be installed on structural elements or buried in them. Actuators

installed on different structural elements may damage due to ductility or inappropriate continuity, but this can be prevented by burying them. However, this action reduces appropriate performance and function of the stimulus because by burying them the stimuli become closer to natural axis of structural elements and produce lower torque compared to the position in which stimuli are installed on the structure. Piezoelectric actuators are usually determined with factors such as free deformation and applied force. Free deformation is calculated in a position where applied voltage is the highest, the actuator is free, and no force is applied. Since this displacement is obtained in the absence of any external load along the piezoelectric actuator axis, it is called free deformation. Applied force is also calculated in a position in which applied voltage is maximum and actuator cannot have the slightest motions, therefore, when displacement is maximum and force is minimum and vice versa. The simplest piezoelectric ceramics can generate very small displacements and very large forces.

3 DERIVING MODELING EQUATIONS

3.1 Constitutive structure

A uniform cantilever beam is determined with rectangular section with determined dimensions.

Timoshenko Theory states that due to applying external load on the beam, perpendicular line to neutral axis would be perpendicular after deformation. Now, the two-dimensional figure of the beam is assumed by considering x as vertical axis and y as transverse axis. According to linear finite elements, the relation between $w(x,t)$ and local coordinates of q are determined by N_w function.

$$w\left(x,t\right)=N_w q \tag{1}$$

Now, by two successive differentiations in terms of x, Eqs. (2) and 3 are obtained from Eq. (1).

$$w'\left(x,t\right)=N_\theta q \tag{2}$$

$$w''\left(x,t\right)=N_a q \tag{3}$$

In order to obtain the speed of each node due to fluctuations, differentiation in terms of t is derived from Eq. (1).

$$\dot{w}\left(x,t\right)=\frac{\partial w}{\partial t}=N_w\ \frac{\partial w}{\partial t}=N_w\ \dot{q} \tag{4}$$

From Eqs. (2) and 3, Eq. (5) can be obtained for shape functions.

$$N_\theta=\frac{\partial N_w}{\partial x} \tag{5a}$$

$$N_a=\frac{\partial^2 N_w}{\partial x^2} \tag{5b}$$

where, N_w, N_θ and N_a are defined for transverse, rotation, and bending displacement, respectively. The objective of using them in potential energy, kinetic energy, and virtual work equations is to extract stiffness, mass, and force matrices [18]. Therefore there is geometrically showing cantilever beam in Fig.1.

Fig.2 is defined shearing effects between Timoshenko beam element and Euler-Bernoulli beam element.

Now, 4 degree of freedom in a element beam is showen in Fig.3.

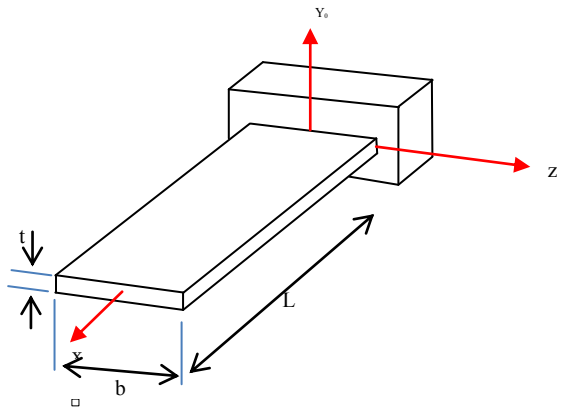

Fig.1
Cantilever beam with rectangular cross-section.

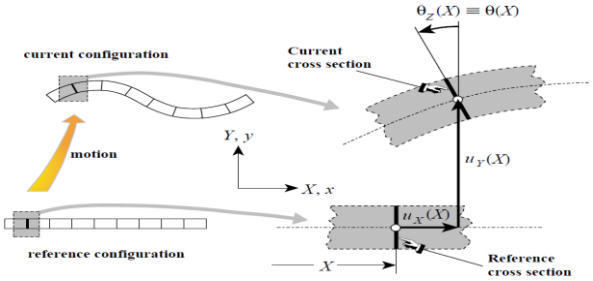

Fig.2
Shearing effects in Timoshenko beam.

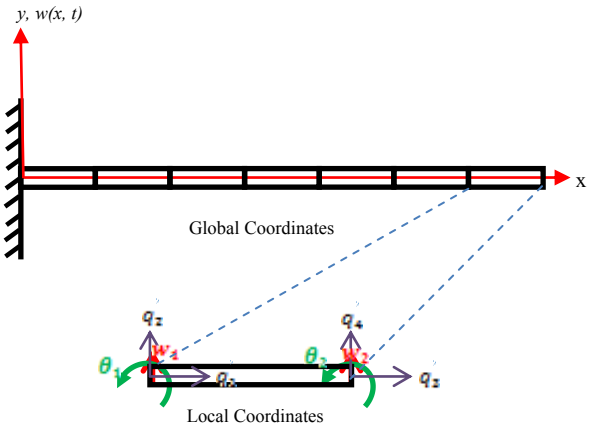

Fig.3
Degree of freedom for every node of elements.

Shape function of transverse displacement

$$\left[N_w\right]^T = \begin{bmatrix} \frac{1}{1+\varphi}\left\{2\left(\frac{x}{l_e}\right)^3 - 3\left(\frac{x}{l_e}\right)^2 - \varphi\left(\frac{x}{l_e}\right) + 1 + \varphi\right\} \\ \frac{1}{1+\varphi}\left\{\left(\frac{x}{l_e}\right)^3 - \left(2+\frac{\varphi}{2}\right)\left(\frac{x}{l_e}\right)^2 - \left(1+\frac{\varphi}{2}\right)\left(\frac{x}{l_e}\right)\right\} \\ \frac{-1}{1+\varphi}\left\{2\left(\frac{x}{l_e}\right)^3 - 3\left(\frac{x}{l_e}\right)^2 - \varphi\left(\frac{x}{l_e}\right)\right\} \\ \frac{1}{1+\varphi}\left\{\left(\frac{x}{l_e}\right)^3 - \left(1-\frac{\varphi}{2}\right)\left(\frac{x}{l_e}\right)^2 - \frac{\varphi}{2}\left(\frac{x}{l_e}\right)\right\} \end{bmatrix} \quad (6)$$

Shape function of rotation displacement

$$\left[N_\theta\right]^T = \begin{bmatrix} \frac{6}{(1+\varphi)l_e}\left\{\left(\frac{x}{l_e}\right)^2 - \left(\frac{x}{l_e}\right)\right\} \\ \frac{1}{(1+\varphi)}\left\{3\left(\frac{x}{l_e}\right)^2 - (4+\varphi)\left(\frac{x}{l_e}\right) + 1 + \varphi\right\} \\ \frac{-6}{(1+\varphi)l_e}\left\{\left(\frac{x}{l_e}\right)^2 - \left(\frac{x}{l_e}\right)\right\} \\ \frac{1}{(1+\varphi)}\left\{3\left(\frac{x}{l_e}\right)^2 - (2-\varphi)\left(\frac{x}{l_e}\right)\right\} \end{bmatrix} \tag{7}$$

Shape function of bending displacement

$$\left[N_a\right]^T = \begin{bmatrix} \frac{6}{(1+\varphi)l_e}\left\{2\frac{x}{{l_e}^2} - \frac{1}{l_e}\right\} \\ \frac{1}{(1+\varphi)l_e}\left\{\frac{6x}{l_e} - (4+\varphi)\right\} \\ \frac{-6}{(1+\varphi)l_e}\left\{2\frac{x}{{l_e}^2} - \frac{1}{l_e}\right\} \\ \frac{1}{(1+\varphi)l_e}\left\{6\frac{x}{{l_e}^2} - \left(\frac{2-\varphi}{l_e}\right)\right\} \end{bmatrix} \tag{8}$$

According to Timoshenko Theory, which considers shear deformation during bending deformation, two sections are provided in kinetic energy, potential energy, and virtual work equations to describe dynamic behavior [18].

Potential energy

$$U = \frac{EI}{2}\int_0^{l_e}\left(\frac{\partial\theta}{\partial x}\right)^2 dx + \frac{KGA}{2}\int_0^{l_e}\left(\frac{\partial w}{\partial x} + \theta\right)^2 dx \tag{9}$$

Kinetic energy

$$T = \frac{\rho A}{2}\int_0^{l_e}\left(\frac{\partial w}{\partial t}\right)^2 + \frac{\rho I}{2}\int_0^{l_e}\left(\frac{\partial\theta}{\partial t}\right)^2 dx \tag{10}$$

Virtual work. Now, Hamilton equation is used to extract stiffness, mass, and force matrices:

$$W_v = \int_0^{l_e} wf dx + \int_0^{l_e}\theta m dx \tag{11}$$

where, mass, stiffness, and force matrices for one element of beam are extracted are extracted as Eqs. (14) and 15:

$$\delta\Pi = \int_{t_1}^{t_2}\left(\delta U - \delta T - \delta W_v\right)dx = 0 \tag{12}$$

Mass matrix for one element of beam

$$M = \rho A \int_0^{l_e} [N_w]^T [N_w] dx + \rho I \int_0^{l_e} [N_\theta]^T [N_\theta] dx \tag{13}$$

Stiffness matrix for one element of beam

$$K = EI \int_0^{l_e} \left[\frac{\partial N_\theta}{\partial x}\right]^T \left[\frac{\partial N_\theta}{\partial x}\right] dx + KGA \int_0^{l_e} \left[[N_\theta] + \left[\frac{\partial N_w}{\partial x}\right]\right]^T \left[[N_\theta] + \left[\frac{\partial N_w}{\partial x}\right]\right] dx \tag{14}$$

And finally, force matrix for one element of beam is shown as Eq. (16).

$$F = \int_0^{l_e} [N_w]^T [f] dx + \int_0^{l_e} [N_\theta]^T [m] dx \tag{15}$$

Eqs. (14)-(15)-(16) are considered as the most fundamental relations in describing dynamic behavior of one element of beam in numerical method of finite element.

3.2 Electromechanical modeling

Fig. 4(a) indicates a cantilever structure with piezoelectric sensor and actuator patches, convertor, magnifying gain, and controller. This smart system actively controls beam vibrations. In order to investigate behavior effect of piezoelectric patches embedded as sensor in the bottom and as actuator at top of the beam, we focus on Fig. 4(b). One element of beam where the piezoelectric sensor and actuator patches are exactly embedded is considered. When the beam is vibrated, the beam is deformed. Stress is applied in the structural element as shear force on piezoelectric sensor patch, leads to piezoelectric sensor and actuator patches deformation, and finally generates electrical voltage. Then, the voltage passes through the convertor, magnifier, and controller. Finally, choosing control gain by the controller, a signal from controller to the magnifier and then from the digital convertor to analog is applied on piezoelectric actuator as voltage. Now, considering the adverse piezoelectric behavior, the actuator would express a strain proportional to voltage. It would prevent from fluctuations and deformation in its placement with actuator by generating strain in the reverse direction of the element motion and attenuate the structure.

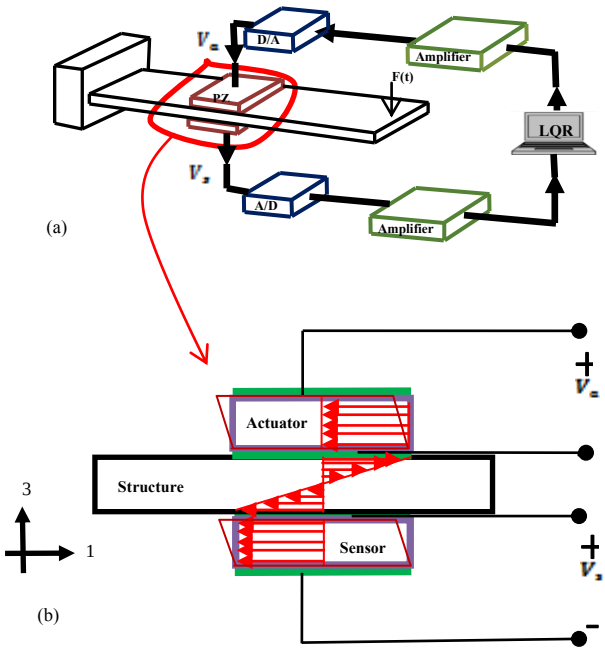

Fig.4
Electromechanical model (a) Smart beam (b) Smart element.

3.3 Assemblage piezo -patches and structures

Stiffness matrices for piezoelectric element are similar to beam structure. The only difference is in mechanical features related to piezoelectric materials. Now, an element beam and piezoelectric patches are installed as sensor and actuator on the bottom and top of the beam according to Fig.5.

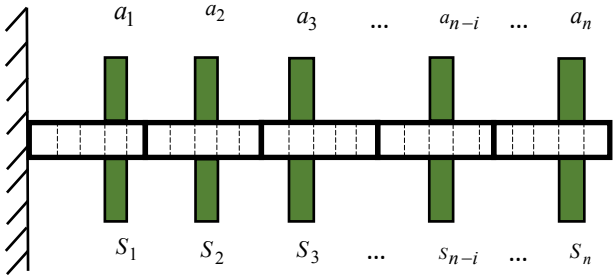

Fig.5
Assemblage piezo-patches on beam.

Sensor and actuator must be assembled with the beam. Obviously, piezoelectric sensor and actuator with beam structure compose a smart structure. Therefore, stiffness and mass matrices are defined as:

$$M_{smart} = Assamblage(M_{beam}, \sum_{i=1}^{n} M_s, \sum_{i=1}^{n} M_a) \tag{16}$$

$$K_{smart} = Assamblage(K_{beam}, \sum_{i=1}^{n} K_s, \sum_{i=1}^{n} K_a) \tag{17}$$

In Eqs. (22) and (23), stiffness and mass matrices are respectively considered for a smart structure.

$$C_{smart} = \alpha M_{smart} + \beta K_{smart} \tag{18}$$

It is considered for smart element with stiffness and mass matrices. Other elements of beam that lack piezoelectric sensor and actuator are assembled through elimination or penalty method [19], which is used in finite element.

3.4 Smart structure

According to Newton's second law for a linear system, dynamic behavior can be described as:

$$M_{smart}\ddot{y} + C_{smart}\dot{y} + K_{smart}y = f_t \tag{19}$$

where, f_t consists of control force from piezoelectric in order to attenuate system and as control force and external force as disturbance applied on the system as external force on the structure. Therefore,

$$f_t = f_{ext} + f_p \tag{20}$$

Control force generated from the piezoelectric actuator is a function of voltage adopted from controller. In order that the actuator would convert the voltage as torque, it should affect the shape function of actuator patch. Therefore, we have Eqs. (21) and (23) [18]:

$$f_p = hV_a \tag{21}$$

$$h = \int_0^{le} N_\theta dx \tag{22}$$

Piezoelectric actuator voltage is a function of mechanical features of piezoelectric material, bending shape function, controller gain, and node speeds on which the piezoelectric actuator is exactly embedded. G_c is related to electrical resistance path voltage from voltage to the actuator. K_{ctrl} is controller gain that is described in next section. Therefore, the voltage applied for this kind of actuator is described as Eq. (23) [18].

$$V_a = K_{ctrl}\left(G_c e_{31} z b \int_0^{l_e} \left[N_a\right]^T dx\right)\dot{q} \tag{23}$$

where $z = \frac{t_b}{2} + t_p$

3.5 LQR controller

Consider Eq. (19) as a dynamic system in the form of Eq. (24) describing a state space.

$$\dot{y} = A_s y + B_s w + E_{ce} u \tag{24}$$

where, matrices *A, B*, and *E* are considered as Eqs. (25)-(26)-(27).

$$A_s = \begin{bmatrix} [0] & [I] \\ -\left[\frac{K_{smart}}{M_{smart}}\right] & -\left[\frac{C_{smart}}{M_{smart}}\right] \end{bmatrix} \tag{25}$$

$$B_s = \begin{bmatrix} [0] \\ \left[\frac{f_e}{M_{smart}}\right] \end{bmatrix} \tag{26}$$

$$E_{ce} = \begin{bmatrix} [0] \\ \left[\frac{f_p}{M_{smart}}\right] \end{bmatrix} \tag{27}$$

In a way that matrix K_{ctrl} is the following optimal control vector.

$$u = -K_{ctrl} y \tag{28}$$

Providing that the following objective function is minimum.

$$J = \frac{1}{2}\int_0^{+\infty} \left(y^T Q y + u^T R u\right) dt \tag{29}$$

where, *Q* is a positive fixed or semi-fixed matrix and *R* is a positive fixed matrix [14]:

$$Q = \begin{bmatrix} \alpha_1 \left[w_i{}^2 \right] & [0] \\ [0] & \alpha_2 [I] \end{bmatrix} \qquad R = \gamma [I] \tag{30}$$

where, a_1, a_2, and γ are optimized and extracted by MOPSO optimizing algorithm based on different locations of piezoelectric sensor and actuator. The range of coefficients of Eq. (30) is introduced to the algorithm as trial and error, providing that the interval recommended to the algorithm would be in the scope of piezoelectric actuators.

3.6 MOPSO algorithm

MOPSO is one of the most common algorithms for smart optimization. This method is able to find the optimal spot. This algorithm the same as other computational techniques for direct search uses a population consisting of potential solutions to the problem to explore the search space. However, the main difference of this method with other methods is that each particle has a velocity vector by which it starts to search. The vector has three components including the particle motion to the best position it has ever found, the best position where a particle of the whole population has reached, and a coefficient of the velocity of previous stage. What has caused fame for particle swarm optimization can be detailed as follows [20]:

This method is almost simple and easy to use. In the original algorithm of particle swarm optimization in contrast to other methods, only one simple actuator is used.

In many applications, particle swarm optimization method is very successful and effective. Therefore, very good results with low computational costs are obtained.

In particle swarm optimization, particles move all along the multi-dimensional search space. The location of each particle changes with the experience of itself and the neighbors [20].

$$\vec{x}_i (t+1) = \vec{x}_i (t) + \vec{v}_i (t+1) \tag{31}$$

Let $\vec{x}_i (t)$ show the i^{th} particle position in time t. The position of the next step with increase in velocity to the current position of the particle is as follows. Velocity vector $\vec{v}_i (t+1)$ is defined with the following equation:

$$\vec{v}_i (t+1) = w\vec{v}_i (t) + C_1 r_1 \left(\vec{x}_{pbest_i} (t) - \vec{x}_i (t) \right) + C_2 r_2 (\vec{x}_{gbest_i} (t) - \vec{x}_i (t)) \tag{32}$$

r_1 and r_2 are random values in [0, 1]. As noted before, w is weight coefficient, and C_1 and C_2 are individual and social learning coefficients, respectively. $\vec{x}_{pbest_i}$ is the best location where the i^{th} particle has reached and $\vec{x}_{gbest_i}$ is the i^{th} guide location. Therefore, particles move by being influenced by other particles to which they are connected. The particles are known as particle neighbors. Schematically, Fig.6 is vectorially is defined particle swarm optimization.

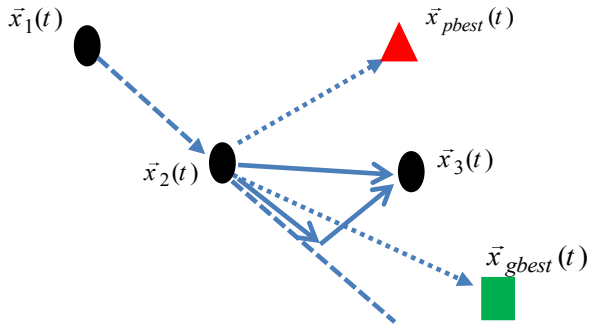

Fig.6
Vector optimization of MOPSO.

3.6.1 MOPSO optimization steps

1) Creating initial population and assessment.
2) Separating non-dominant members and storing the in archive.
3) Tabulating the guided space.
4) Each particle among archive members is chosen a leader and continues to move.
5) The best individual memory of particles is chosen.
6) Non-dominant members of the archive are removed.
7) If the number of archive members is more than the defined capacity, the extra members are removed and tabulation is renewed.
8) If the termination condition is not met, return to step 3; otherwise finish.

By considering the references, optimal weights of 31 and 32 equations have been adopted based on Ref. [21].

$$\phi_1 = \phi_2 = 2.05 \tag{33}$$

$$\phi = \phi_1 + \phi_2 \tag{34}$$

$$\chi = \frac{2}{\left(\phi - 2 + \sqrt{\phi^2 - 4\phi}\right)} \tag{35}$$

$$w = \chi \tag{36}$$

$$C_1 = \chi\phi_1 \tag{37}$$

$$C_2 = \chi\phi_2 \tag{38}$$

3.6.2 How to choose leader?

1) Archive members are determined.
2) Tabulation is done optionally.
3) The cell with lower population is chosen.
4) One of the members of the chosen cell is chosen randomly.

4 SIMULATION INPUTS

4.1 Description 1PZT-5PZT models

Simulation on a cantilever beam is presented and compared as Model 2. 1PZT Model is a model that researcher controlled for finding the optimization location to attenuate structure vibrations in the recent decade of modeling. 5PZT is a model suggested for structure vibrations attenuation. 5PZT Model is inspired by 1PZT. The only difference is that in 1PZT, only one pair of sensor and actuator was used, but by dividing the pair to five smaller patches, i.e. 5PZT Model, there has been an attempt to find optimal location for placing piezoelectric sensor and actuator. As can be seen in Fig. 7, these two models are indicated. The characteristics are as follows:

1PZT Model Characteristics

1. Dividing the beam into 20 elements.
2. Beam element length equal to piezoelectric length.

5PZT Model Characteristics

1. Dividing beam to 100 elements.
2. Dividing piezoelectric element into 5 smaller elements.

In this simulation, the objective is to control the first 5 modes of beam vibration. The reason to divide the piezoelectric patch into 5 equal patches in 5PZT Model was to attenuate the first 5 modes of beam vibration. Fig. 8 is a schematic of the fifth mode of cantilever beam vibration. As can be seen from Fig. 8, sensor and actuator

patches are on the spots where the most strain energy has happened. When beam is under fluctuation, infinite vibration modes happen in the beam. Now by using model reduction method, it has been assumed that only the first 5 modes happen in the beam. Now, in order to be conservative and control all the 5 modes, a pair of piezoelectric sensor and actuator in model 1PZT is divided into 5 pairs of smaller patches to detect optimal spots with greater sensitivity. Therefore, that approach is suggested as Fig.7. Clearly, fifth vibration mode is shown as Fig.8.

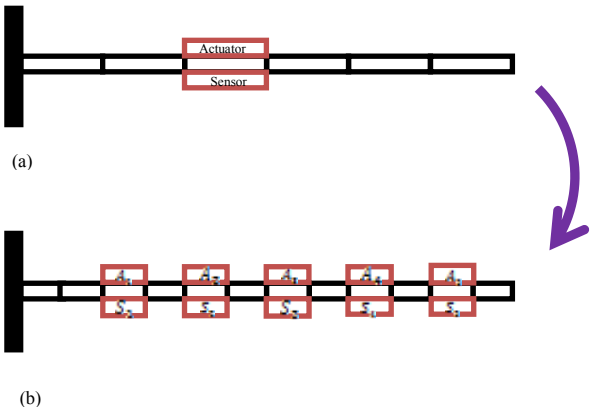

Fig.7
Smart beam model (a) 1PZT (b) 5PZT.

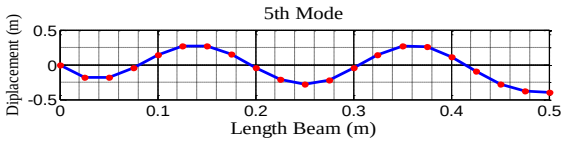

Fig.8
Fifth vibration modes beam.

According to Tables 1and 2, mechanical and geometric properties of the beam and piezoelectric patches used in the simulation are presented.

Table 1
Beam information.

Beam		
Symbol	Parameters	Values
L	Length	0.5 *m*
b_b	Width	0.024 *m*
E_b	Young's Modulus	193.096 *GPa*
ρ_b	Density	8030 Kg / m^3
α & β	Damping Constants	0.001 & 0.0001
t_b	Thickness	1 *mm*

Table 2
Piezo - Patch information [18].

Natural Frequency (*Hz*)		
Analytical	Numerical	ANSYS
16.706	16.696	16.698
104.699	104.572	105.01
292.751	292.528	296.26
572.186	572.467	587.65
942.512	944.736	987.59
1402.112	1408.498	1506.4
1949.703	1962.947	2157.4
2584.256	2607.317	2957.5
3304.567	3340.965	3926.8

In locating process under square, Sinusoidal, and pulse inputs, 2 criteria in cost function to find the optimal spot for locating piezoelectric sensor and actuator are considered for two models.

1.Reduced maximum displacement.

2.Reduced maximum voltage of the piezoelectric actuator.

Table 3
Natural frequencies for 9 modes in Timoshenko beam.

PZT		
Symbol	Parameters	Value
l_{pzt}	Length	0.125 m
b_{pzt}	Width	0.024 m
t_{pzt}	Thickness	0.5 mm
E_{pzt}	Young's Modulus	68 GPa
ρ_{pzt}	Density	7700 Kg/m^3
d_{31}	Strain Constant	$125\times10^{-12} m/V$
g_{31}	Stress Constant	$10.5\times10^{-13} Vm/N$

4.2 Pulse input

Pulse input for control systems 1PZT and 5PZT are as Fig. 9.

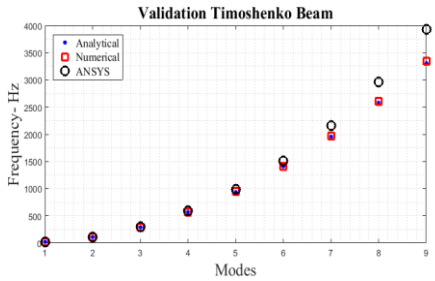

Fig.9
Camparison naturel frequencies of Timoshenko beam.

External disturbance of the beam due to pulse input is described as Fig. 10. Pareto front for models 1PZT and 5PZT are as Fig. 11 using MOPSO.

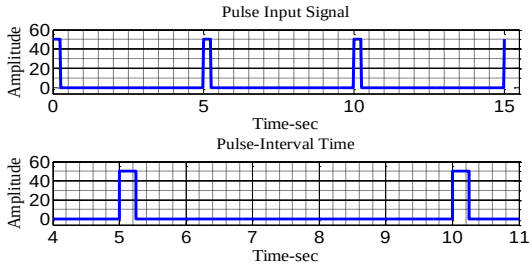

Fig.10
Pulse input value.

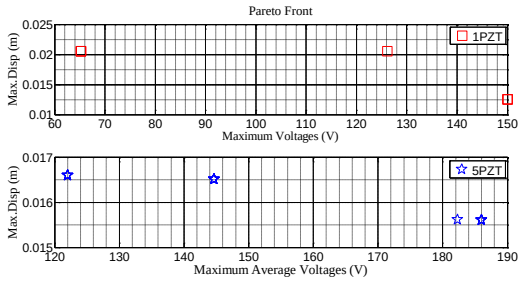

Fig.11
Pulse input of pareto front.

By making logarithm of horizontal axis (time), flexural displacement due to pulse input for tip of the beam would be as Fig. 12.

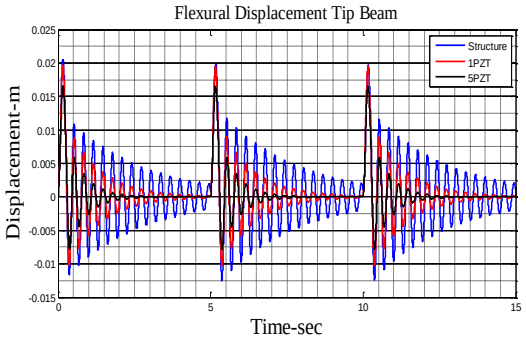

Fig.12
Pulse flexural displacement.

Angular displacement of tip of the attenuated beam in two models of smart beam is shown in Fig. 13.

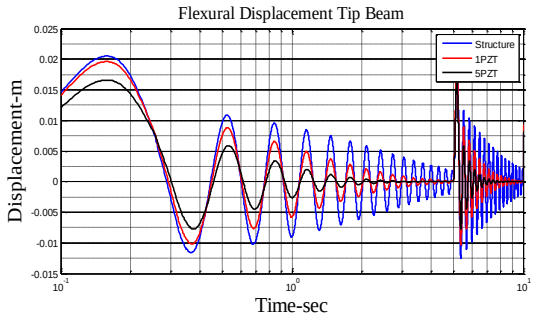

Fig.13
First seconds pulse flexural displacement.

The starting point of pulse input for angular displacement of tip of the beam for models 1PZT and 5PZT are as Fig. 14. Fig.15 is logarithmically defined Fig.14 correctly as can show:

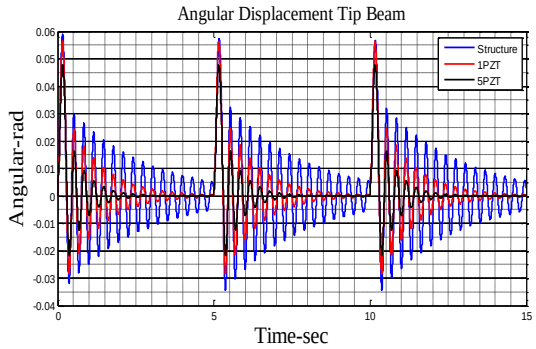

Fig.14
Pulse angular displacement.

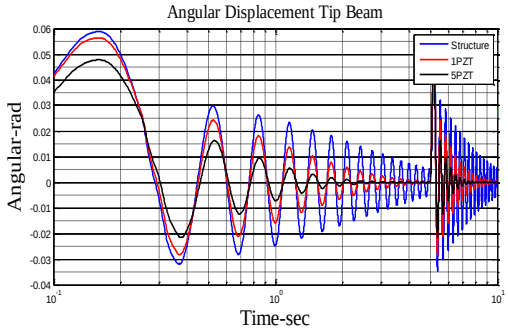

Fig.15
First seconds pulse angular displacement.

Using MOPSO algorithm, the optimized values are as Table 4.

Table 4
Optimal values of pulse input.

		1 PZT	5 PZT
Objectives	Max.Voltage(V)	32.614	122.0047
	Max.Disp.(m)	2.05×10^{-2}	1.65×10^{-2}
	Element Location	10	[3,92,37,2,50]
LQR	α_1	99.617	95.421
	α_2	8.739	76.335
	γ	0.4075	0.0592

Input optimized to piezoelectric for two models is like this. Moreover, productive forces by piezoelectric actuators for the two models are as Fig. 16.

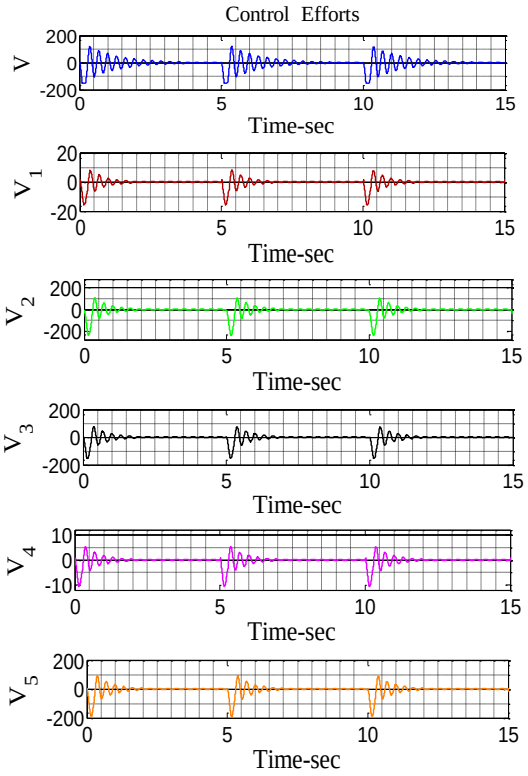

Fig.16
Pulse voltage actuators for 1PZT-5PZT models.

4.3 Sinusoidal input

Sinusoidal input for control systems 1PZT and 5PZT are as Fig. 17.

By applying alternative sinusoidal input on the tip of the beam, Pareto optimized by algorithm based on 2 optimized voltage criteria of piezoelectric actuator and maximum displacement of the beam is as Fig. 18.

As can be seen in Fig. 19, structure vibration faces with increase in displacement and reaches a fixed amount after 10 seconds. The main reason is that the structure has its transient response until the 10^{th} second and it then reaches the steady state response.

Flexural displacement in the tip of the beam due to Sinusoidal input is shown in Fig. 20.

Sinusoidal input is used secon input simulation in this section as can show in Fig.18. Pareto front optimal particles are extracted by MOPSO as Fig.19

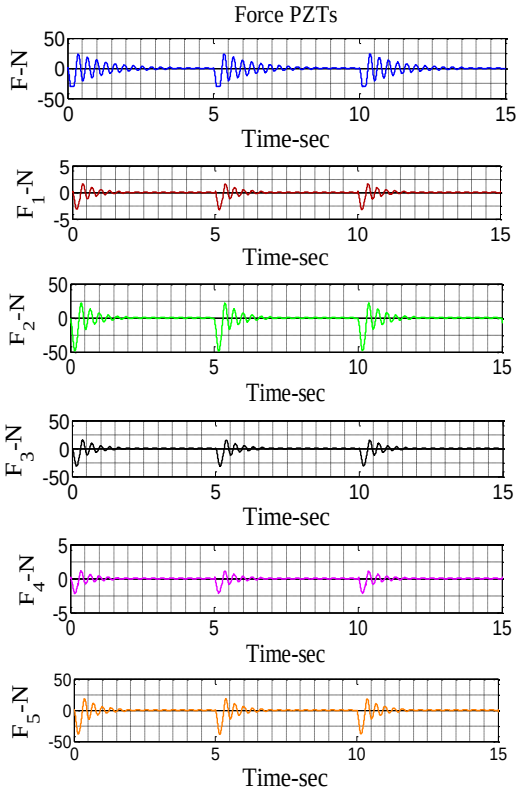

Fig.17
Pulse force actuators for 1PZT-5PZT models.

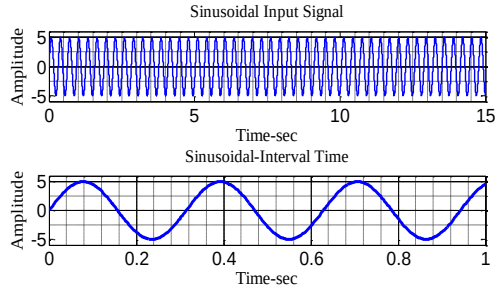

Fig.18
Sinusoidal input value.

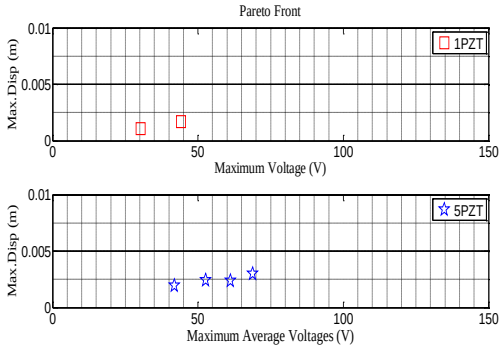

Fig.19
Sinusoidal input of pareto front.

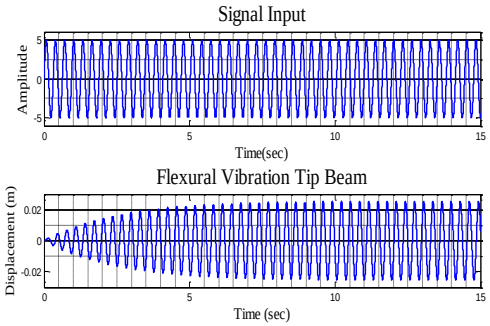

Fig.20
Comparison input and output.

In order to concentrate on design of the models, at the initial moment and by applying Sinusoidal input, the time axis logarithm is made and Fig. 21 is displayed.

Angular displacement of the tip of the beam in Sinusoidal input is as Fig. 22. And also, it is shown flexural displacement of first second mode for 2 term such as transient and forced response as Fig.22. Initial moment of Sinusoidal input for angular displacement is as Fig. 23. Angular displacement is another degree of freedom in tip beam element as Fig.23.

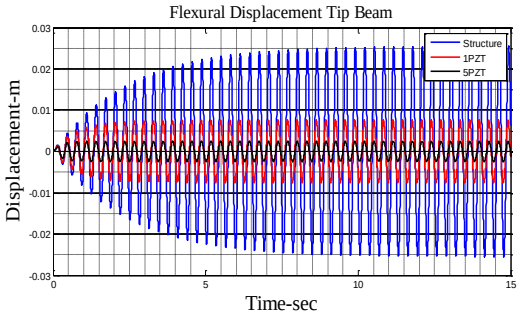

Fig.21
Sinusoidal flexural displacement.

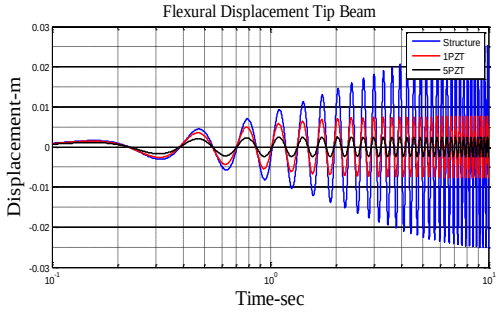

Fig.22
First seconds sinusoidal flexural displacement.

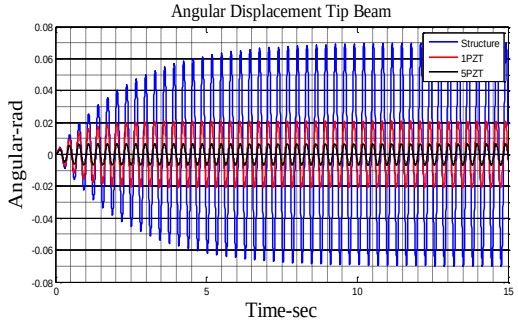

Fig.23
Sinusoidal angular displacement of tip beam.

In Table 5., optimal amounts of LQR controller coefficients, location, maximum voltage, and displacement of tip of the beam have been extracted by the algorithm.

Table5
Optimal values of sinusoidal input.

		1 PZT	5 PZT
Objectives	Max.Voltage(V)	30.259	52.677
	Max.Disp(m)	2.67×10^{-3}	2.43×10^{-3}
Element Location		16	[77,81,87,9,40]
LQR	α_1	56.147	11.558
	α_2	3.118	96.227
	γ	0.443	0.0132

According to reference [6] that has used the same piezo ceramic sensor and actuator for beam attenuation, for 0.5 *mm* thickness of piezo ceramic it has the maximum voltage capability of 500 *volts*. As can be seen in Fig. 24, the applied voltages on piezo ceramic actuators with thickness of 0.5 *mm* (according to Table 2.) have been in the work scope of actuators. Performance of optimized voltages in 1PZT and 5PZT that have been found with optimization algorithm is as Fig. 24.

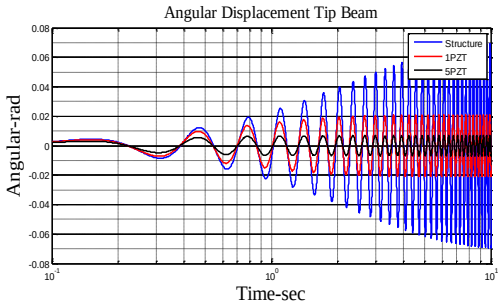

Fig.24
First seconds sinusoidal angular displacement.

Moreover, forces generated by piezoelectric for the two models are as Fig. 25.

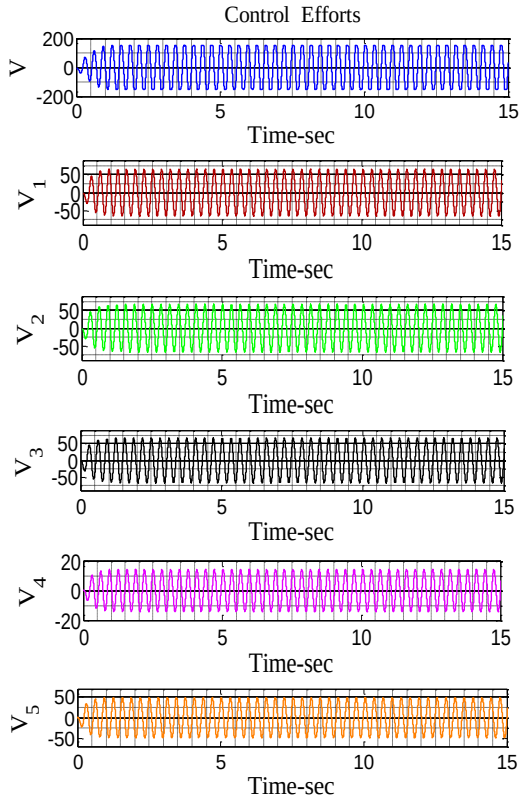

Fig.25
Sinusoidal voltage actuators for 1PZT-5PZT models.

4.4 Square Input

Square input for control systems 1PZT and 5PZT is as Fig. 26.

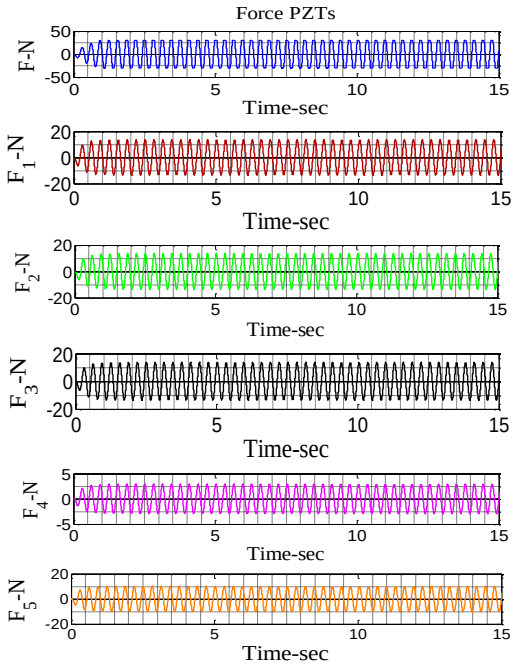

Fig.26
Sinusoidal force actuators for 1PZT-5PZT models.

Pareto front of Fig. 27 for the 2 models for Square input has been extracted as follows.

As can be seen in Fig.28, flexural displacement of the tip of the beam is due to square dynamic load on the beam. And also optimal particles is exploited as can present in Fig.28.

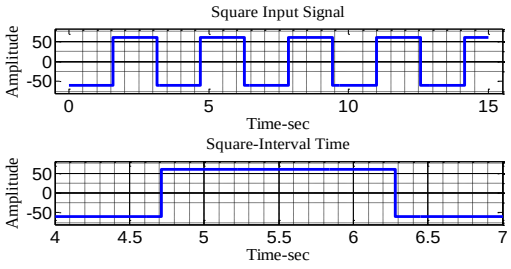

Fig.27
Square input value.

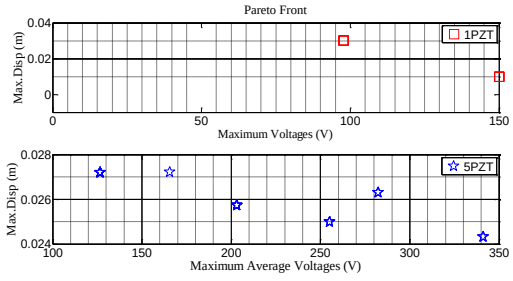

Fig.28
Square input of pareto front.

At the beginning of the effect of square input on the beam, flexural displacement of the models is as Fig. 29.

Angular displacement of the tip of the beam in square input can be seen in Fig. 30. Logarithmically, Fig.29 is drawn in Fig.30 for first second mode.

For more accuracy in Fig. 30, the initial time of square input on the beam is considered as Fig. 31. Fig.31 is shown based on square input.

Optimized control effort on piezoelectric disablement in the models is shown as Fig.32. First second mode of angular displacement is logarithmically shown in Fig.32.

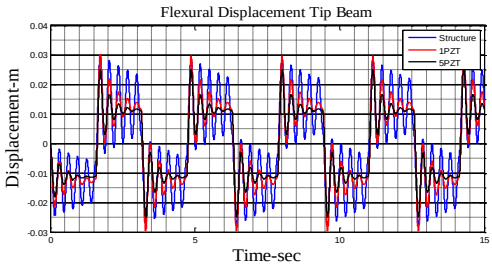

Fig.29
Square flexural displacement.

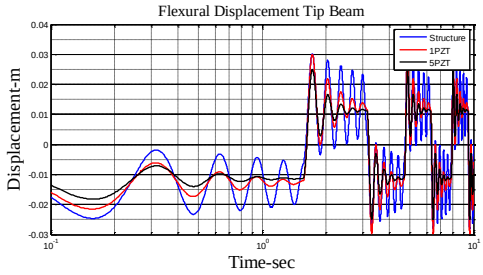

Fig.30
First second square flexural displacement.

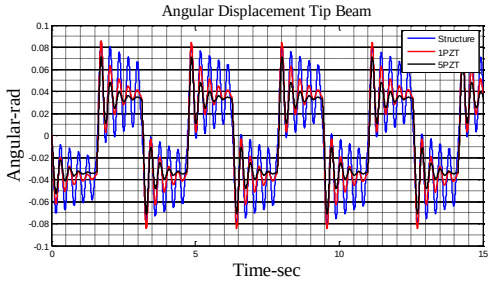

Fig.31
Square angular displacement.

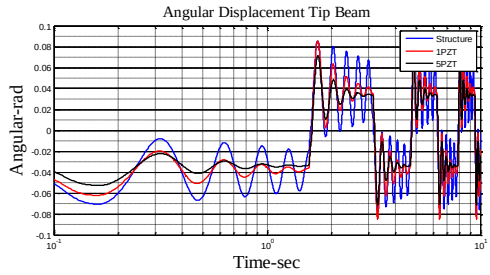

Fig.32
First second square angular displacement.

Optimal values of square input on the beam are as Table 6.

Table 6
Optimal values of square input.

		1 PZT	5 PZT
Objectives	Max.Voltage(V)	97.753	126.492
	Max.Disp (m)	3.01×10^{-2}	2.71×10^{-2}
Element Location		12	[2,49,20,38,37]
LQR	α_1	35.547	95.113
	α_1	6.315	37.959
	γ	0.0515	0.5229

Moreover, forces generated by piezoelectric actuators for the models are shown as Fig. 33. Piezoelectric force actuators are presented as Fig.34.

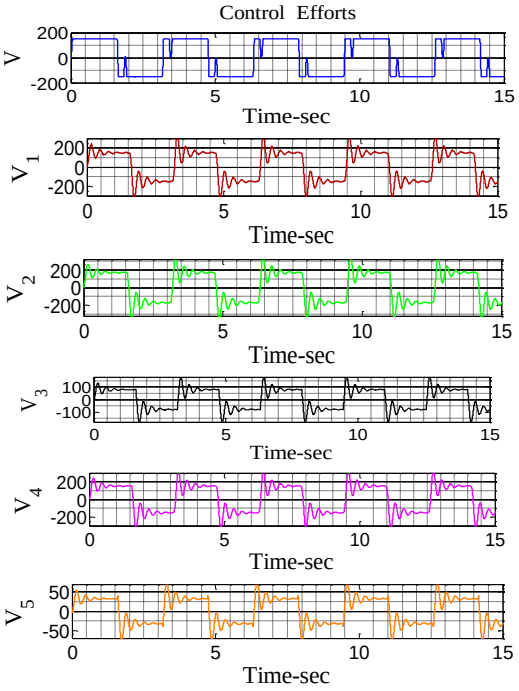

Fig.33
Square voltage actuators for 1PZT-5PZT models.

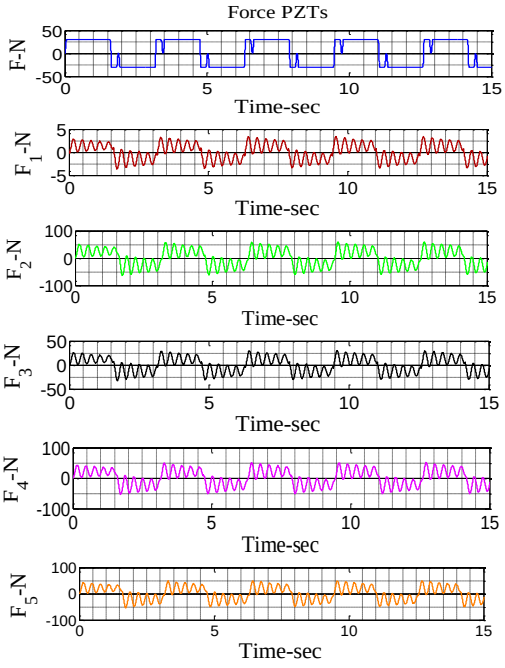

Fig.34
Square force actuators for 1PZT-5PZT models.

5 CONCLUSIONS

1. Increasing the number of piezoelectric patches has a significant effect on detecting critical points.
2. 5PZT model has a more optimal attenuation compared to 1PZT.
3. More vibration modes can be controlled with 5PZT rather than 1PZT.

4. Minimum vibration attenuation time compared to 1PZT due to lower power loss
5. According to γ, 5PZT compared to 1PZT in Sinusoidal, Pulse, and Step inputs has cheaper control. In contrast, square input in 1PZT has cheaper control compared to 5PZT.
6. According to reference [6], the voltage of actuators in 5PZT and voltage of actuators in 1PZT are logical and feasible values.
7. Response duration of sinusoidal input in 5PZT is less than 1PZT. This means to reach a faster persistent response with vibration amplitude in 5PZT model.
8. According to locating piezoelectric patches on the beam, stiffness and mass change and this leads to beam displacement. This can be observed in all charts drawn with logarithmic horizontal axis.
9. The main reason for increase in amplitude and reaching a fixed amount of displacement in sinusoidal input (Fig. 20) is that state space model is used to explain dynamic behavior of the beam, and one characteristic of state space model is transient and steady behavior expression of system simultaneously, i.e. the system has transient behavior until 10 seconds and then by fixing displacement, steady behavior appears in the system.
10. Despite designing an LQR controller for 5 pairs of piezoelectric sensor and actuator element in 5PZT, MOPSO determined controller coefficients so that 5 pairs of piezoelectric sensor are covered for vibration attenuation of the beam structure and present a significant attenuation compared with 1PZT.
11. Negative voltage in piezoelectric actuator input indicates positive displacement of the tip of the beam (upward displacement) and positive voltage in actuators indicates negative displacement of the tip of the beam (downward displacement).
12. By observing figures related to piezoelectric actuator voltage (optimized tables extracted from optimizing operation) in pulse, square, and sinusoidal inputs it can be understood that locations determined by MOPSO algorithm is in the beginning of the beam and close to backrest and fewer voltages are deployed compared to elements that are far from the backrest. When the transverse load force is closer to the backrest, less displacement would happen.
13. If location coordinates of the elements determined by MOPSO in 1PZT is mapped to location coordinates in 5PZT, it can be seen that location coordinates are different in 1PZT and 5PZT. The main reason of the difference is the beam physics due to dividing one pair of piezoelectric element into 5 pairs of smaller elements and locating them along the beam, which leads to change in beam stiffness and mass, and finally change in dynamic behavior of the beam.
14. Since the system is considered as linear and we know that in linear systems, input and output are different only in amplitude and phase, this concept is established in them by applying various inputs on the system, and this shows the appropriateness of the modeling. In other words, it also increases the trust on optimal locating approach design.
15. Due to describing system as state space (time area) when a sinusoidal input is applied on the system, persistent response and transient response of the system are shown simultaneously.

REFERENCES

[1] Quek S.T., Wang S.Y., Ang K.K., 2003, Vibration control of composite plates via optimal placement of piezoelectric patches, *Journal of Intelligent Material Systems and Structures* **14**: 229-245.

[2] Liu W., Hou Z., Demtriou M.A.,2006, A computational scheme for the optimal sensor/actuator placement of flexible structures using spatial H_2 measures, *Mechanical System and Signal Processing* **20**: 881-895.

[3] Gua H.Y., Zhang L., Zhang L.L., Zhou J.X., 2004, Optimal placement of sensors for structural health monitoring using improved genetic algorithms, *Smart Material and Structures* **13**: 528.

[4] Rocha da T.L., Silva da S., Lopes Jr V., 2004, Optimal location of piezoelectric sensor and actuator for flexible structures, *11th International Congress on Sound and Vibration*, Petersburg, Russia.

[5] Santoes e Lucato S.L.D., Meeking R.M., Evans A.G., 2005, Actuator placement optimization in a kagome based high authority shape morphing structure, *Smart Materials and Structures* **14**: 86-75.

[6] Brasseur M., Boe P.D., Gdinval J.C., Tamaz P., Caule P., Embrechts J.J., Nemerlin J., 2004, *Placement of Piezoelectric Laminate Actuator for Active Structural Acoustic Control*, University of Twente.

[7] Ning H.H., 2004,Optimal number and placements of piezoelectric patch actuators in structural active vibration control, *Engineering Computations* **21**(6): 601-665.

[8] Oliveira A.S., Junior J.J.L., 2005, Placement optimization of piezoelectric actuators in a simply supported beam through SVD analysis and shape function critic point, *6th World Congress of Structural and Multidisciplinary Optimization*, Brazil.

[9] Wang S.Y., Tai K., Quek S.T., 2006, Topology optimization of piezoelectric sensors/actuators for torsional vibration control of composite plates, *Smart Materials and Structures* **15**: 253-269.
[10] Lottin J., Formosa F., Virtosu M., Brunetti L., 2006, About optimal location of sensors and actuators for the control of flexible structures, *Research and Education in Mechatronics*, Stockholm, Sweden.
[11] Lottin J., Formosa F., Virtosu M., Brunetti L., 2006, Optimization of piezoelectric sensor location for delamination detection in composite laminates, *Engineering Optimization* **38**(5): 511-528.
[12] Belloli A., Ermanni P., 2007, Optimum placement of piezoelectric ceramic modules for vibration suppression of highly constrained structures, *Smart Materials and Structures* **16**: 1662-1671.
[13] Qiu Z.C., Zhang X.M., Wu H.X., Zhang H.H., 2007, Optimal placement and active vibration control for piezoelectric smart flexible cantilever plate, *Journal of Sound and Vibration* **301**: 521-543.
[14] Roy T., Chakraborty D., 2009, GA-LQR based optimal vibration control of smart FRP composite structures with bonded PZT patches, *Journal of Reinforced Plastics and Composites* **28**:1383-1404.
[15] Safizadeh M.R., Mat Darus I.Z., Mailah M., *Optimal Placement of Piezoelectric Actuator for Active Vibration Control of Flexible Plate*, Faculty of Mechanical Engineering University Technology Malaysia (UTM) 81310 Skudai, Johor, Malaysia.
[16] Yang J.Y., Chen G.P., 2010, Actuator placement and configuration direct optimization in plate structure vibration control system, *International Conference on Measuring Technology and Mechatronics Automation*.
[17] Yang J., Chen G., 2010, Optimal placement and configuration direction of actuators in plate structure vibration control system, *2nd International Asia Conference on Informatics in Control, Automation and Robotics*.
[18] Manjunath T.C., Bandyopadhyay B., 2009, Vibration control of Timoshenko smart structure using multirate output feedback based discrete sliding mode control for SISO systems, *Journal Sound and Vibration* **326**: 50-74.
[19] Logan D.L., 2012, *A First Course in the Finite Element Method*, Cengage Learning, Amazon.
[20] Clerc M., 2005, *Particle Swarm Optimization*, ISTE.
[21] Clerc M., Kennedy J., 2002, The particle swarm-explosion stability and convergence in a multidimensional complex space, *IEEE Transaction on Evolutionary Computation*.